Coupled Pitch and Heave Porpoising Instability in Hydrodynamic Planing

Peter R. Payne*
Payne Inc., Annapolis, Md.

"Porpoising" is a form of longitudinal instability characterized by an unstable coupling between heave and pitch degrees of freedom. In connection with flying boat stability, it was first analyzed by Perring and Glauert.[2] In this paper, a simple theoretical description is first presented, based on quasi-static forces and moments, to show that stability is a function of center of gravity (c.g) location with respect to the center of pressure; and to a lesser extent, on the longitudinal radius of gyration. It is found that there are two stable zones; one where the c.g. is well forward of the center of pressure (analogous to a longitudinally stable aeroplane), and a second with the c.g. close to the trailing edge, which has no parallel in aircraft stability theory. Buoyancy terms are found to have a favorable effect for all c.g. positions, so that porpoising is essentially a high speed phenomenon, when most of the weight is supported by dynamic forces. Expressions are then developed for the transient hydrodynamic forces due to heave and pitch rates and accelerations, and the complete pitch and heave equations of motion are studied in some detail. It is concluded that there are several different ways of achieving stability, only one of which (moving the c.g. forward) is intuitively obvious. Other solutions include moving the c.g. right aft, the use of a very large radius of gyration in relation to the length of the planing surface, and the use of a high aspect ratio planing surface. All of these solutions can be identified in successful high-speed boats and hydroplanes. The calculations in the main body of the report assume that the fluid is inviscid. It can be shown (the calculations are omitted for brevity) that skin friction on the planing bottom results in additional terms in the stability equations, but that these are an order of magnitude less than the inviscid terms for a typical planing hull. But at very high speeds, coupled with a high c.g. position, the skin friction term in the pitching moment equation can become important, and may then have a dominant effect on stability. Generally, skin friction terms increase static stability and degrade dynamic stability. Despite the many porpoising tests made in the past with specific flying boat designs, there is very little experimental data available for simple planing surfaces alone; in fact, only the work of Day and Haag[12] is known to the writer. A comparison between the theory and their experimental data gives reasonable agreement under the circumstances, but also points to the need for more experimental work.

Nomenclature†

A = a coefficient of the characteristic equation, defined in the text or, in Table 1, aspect ratio.
a_n = manipulative constants defined in the text
B = a coefficient of the characteristic equation, defined in the text
b = total plate width of a planing plate
b_n = manipulative constants defined in the text
C = a coefficient of the characteristic equation, defined in the text
$\bar{C}_H$ = ratio of uncoupled heave mode damping to the critical value for dead-beat motion
$\bar{C}_P$ = ratio of uncoupled pitch mode damping to the critical value for dead-beat motion
C_τ = $F_D/1/2\,\rho u_0{}^2\pi b^2$, the dynamic force coefficient
c_n = manipulative constants defined in the text
D = a coefficient of the characteristic equation, defined in the text, or total resistance, as in "lift/drag" ratio L/D
D_P = pressure drag force on a planing surface
E = a coefficient of the characteristic equation, defined in the text
F = Froude number based on wetted length = $u_o/(gl_m)^{1/2}$
F_D = the dynamic component of the normal force, due to the plate's velocity through the water
F_H = the hydrostatic component of the normal force
F_N = normal force acting on a planing plate (Fig. 1) = $F_D + F_H$
f = $F^2\tau_o = u_o{}^2\tau_o/gl_{mo}$, a loading parameter
g = acceleration due to gravity
h_G = height of c.g. above the plate surface in contact with the water, measured normal to the plate (Fig. 1)
I = moment of inertia about the c.g. in pitch = $Wr_G{}^2/g$
i = propulsor thrust line inclination to the planning surface (Fig. 12)
K_D = $1/2\,\rho u_o{}^2\pi b^2\,1/2[l_{mo}/(b+l_{mo})] = F_{Do}/\tau_o$
K_H = $1/2\,\rho g b l_{mo}{}^2 = F_{Ho}/\tau_o$
L = lift, as in "lift/drag" ratio L/D. $L \simeq F_N$
l_G = distance between the c.g. and the aft edge of the plate, measured parallel to the plate (Fig. 1)
l_m = plate wetted length, defined in Fig. 1
$\hat{l}$ = $\Delta l/l_{mo}$, the nondimensionalized small perturbation in wetted length
$\bar{l}$ = Laplace transform of $\hat{l}$
M = moment about the c.g. due to normal water forces acting on the plate
M_o = moment acting about the c.g. due to forces other than those actong on the plate, such as propeller thrust or aerodynamic forces
m' = virtual or associated water mass per unit length of plate
p_1 = propulsor distance below the planning surface (Fig. 17)
p_2 = propulsor distance behind the planing surface trailing edge (Fig. 17)
R = $r_G/l_G = \dfrac{\text{radius of gyration}}{\text{distance between c.g. and plate trailing edge}}$
r_G = radius of gyration in pitch about the c.g. = $(Ig/W)^{1/2}$
s = the complex variable of the Laplace transformation
T = propulsor thrust (Fig. 17)
t = time
$\hat{t}$ = $u_o t/l_{mo}$, a nondimensional time parameter
u_o = steady-state velocity of the plate across the water
W = total boat weight
x = distance from the c.g. aft, measured along the plate (Fig. 1)
x_H = $l_G - 1/3 l_m$
x_m = $l_G - l_m$
x_η = distance between the c.g. and the center of pressure of the normal force, measured parallel to the plate's surface

Received November 13, 1973; revision received December 4, 1973.
Index categories: Marine Hydrodynamics, Vessel and Control Surface; Marine Vessel Trajectories, Stability, and Control.
*President. Member AIAA.
† Differentiation with respect to time is denoted by dots, in the Newtonian manner. Differentiation with respect to the reduced time parameter $\hat{t}$ is denoted by acute accents; thus: τ.

y = height of the boat's c.g. above the undisturbed water surface.
β = deadrise angle of a V-bottom planing surface
$\gamma = gm'l_{mo}/W = gM'/W =$ weight of virtual mass of water / weight of the boat
ΔF_T = component of the normal force due to transient motion
Δl = small wetted length perturbation from the steady trim value l_{mo}
ΔM_T = component of the normal force moment about the c.g. due to transient motion
$\Delta\tau$ = small trim angle perturbation from the steady trim value τ_o
δ = "hook angle," defined in Fig. 27
$\lambda = F_H/W = F_H/(F_H + F_D)$, the ratio of hydrostatic to total normal force on the plate
ρ = mass density of the water
τ = trim angle of the plate (Fig. 1)
$\hat{\tau} = \Delta\tau/\tau_o$, a small perturbation trim parameter
$\bar{\tau}$ = Laplace transform of $\hat{\tau}$
$\phi = l_G/l_{mo} =$ c.g. distance forward of the trailing edge / wetted length
$\psi =$ dynamic normal force on a planing surface with deadrise / dynamic normal force on a flat plate at the same trim angle
ω_H = natural frequency (rads/sec) of the uncoupled heave motion
ω_P = natural frequency (rads/sec) of the uncoupled pitch motion

Introduction

MANY seaplanes and high-speed planing boats experience porpoising at some combination of speed and trim angle. Porpoising may be described as a form of longitudinal dynamic instability, characterized by a coupled heave and pitch angle motion.‡ It can result in the destruction of a lightly built seaplane or flying boat, although planing boat operators will generally find, if they persevere, that such unstable motions are amplitude limited (rather like an electronic oscillator) and that the motion is usually not violent enough to damage a well-built hull except at very high speeds. Nevertheless, such instability is clearly undesirable, and in practice it is eliminated or minimized by changing the location in the boat of the major weight items. For example, Savitsky[1] states that the practical rule of thumb is to move the c.g. forward and/or reduce the trim angle by means of a shingle or downwardly deflected tab at the transom.

Such empiricisms rarely cover all cases, unfortunately. Thus, it was decided to analyze the simplest possible case of a planing flat plate, in order to gain insight into the basic causes of porpoising instability.

The only previous analysis of the subject is due to Perring and Glauert[2] (1932) who considered the total problem of seaplane porpoising.§ Their expression for the normal force on a single planing surface was

$$F_D = \frac{1}{2}\rho u_o^2 b l_m \tau$$

implying

$$C_\tau = \frac{F_D}{(1/2)\rho u_o^2 \pi b^2} = \frac{1}{\pi}\left(\frac{l_m}{b}\right)$$

This is very similar to modern formulations of planing lift. In the present paper, we use Shuford's relationship

$$C_\tau = \frac{1}{2}\frac{l_m}{b}\Big/\left(1 + \frac{l_m}{b}\right) \qquad (1)$$

Perring and Glauert[2] did not account for buoyant forces on the planing surface, and since they were concerned with the total seaplane problem, involving aerodynamic as well as hydrodynamic forces, they did not study the stability of the planing plate alone. Nor did they attempt to estimate the dynamic forces due to transient motion $(\dot{\tau},\ddot{\tau},\dot{y},\ddot{y})$ of the plate.

‡It is analogous in many ways to binary flutter, where wing torsion and flap couple together.

§The theory of Perring and Glauert was applied to a particular seaplane by Klemin, Pierson, and Storer in Ref. 13.

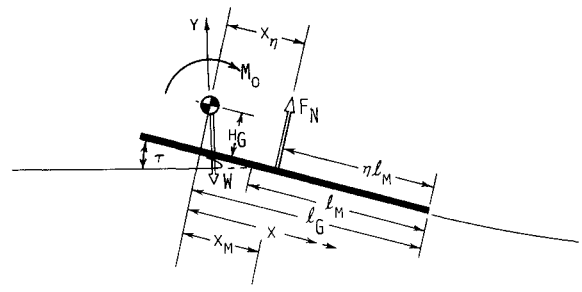

Fig. 1 A simple planing plate.

Theory

"Porpoising" occurs in towing tank experiments where the model is free to pitch and heave, but has no other degrees of freedom. Thus, only pitch and heave will be considered in this analysis.

Confining the analysis to small angles ($\tau \ll 1$) we initially neglect all transient water pressure terms. The center of lift is taken to be a fraction η of the nominal wetted length (l_m), forward of the trailing edge.

It is also convenient to linearize the problem by the method of small perturbations, so that we require the following definitions:

$$\left.\begin{aligned} y &= h_G + x_m\tau \\ \therefore\ \dot{y} &= \dot{x}_m\tau + x_m\dot{\tau} \\ \ddot{y} &= \ddot{x}_m\tau + 2\dot{x}_m\dot{\tau} + x_m\ddot{\tau} \\ \tau &= \tau_o + \Delta\tau \\ x_m &= l_G - (l_{mo} + \Delta l) = x_{mo} - \Delta l \\ x_\eta &= l_G - \eta(l_{mo} + \Delta l) = x_{\eta o} - \eta\Delta l \\ x_H &= l_G - \frac{1}{3}(l_{mo} + \Delta l) = x_{Ho} - \frac{1}{3}\Delta l \end{aligned}\right\} \qquad (2)$$

As is usual, only the linear terms in $\Delta\tau$, Δl and so on will be retained in the analysis.

We write the dynamic normal force as

$$\begin{aligned} F_D &= \frac{1}{2}\rho u_o^2\pi b^2\,\frac{1}{2}\left(\frac{l_m}{b + l_m}\right)\tau \\ &= \frac{1}{2}\rho u_o^2\pi b^2\,\frac{1}{2}\left(\frac{l_{mo}}{b + l_{mo}} + \frac{\Delta l}{b + l_{mo}}\right)(\tau_o + \Delta\tau) \\ &= K_D\tau_o + K_D\Delta\tau + K_D\tau_o(\Delta l/l_{mo}) \end{aligned} \qquad (3)$$

where $K_D\tau_o = F_{Do}$, the trim value and

$$K_D = (1/2)\rho u_o^2\pi b^2(1/2)[l_{mo}/(b + l_{mo})]$$

For the hydrostatic normal force component

$$\begin{aligned} F_H &= \frac{1}{2}\rho g b(l_{mo} + \Delta l)^2(\tau_o + \Delta\tau) \\ &= K_H\tau_o + K_H\Delta\tau + 2K_H\frac{\tau_o}{l_{mo}}\Delta l \end{aligned} \qquad (4)$$

where $K_H\tau_o = F_{HO}$, the trim value, and

$$K_H = (1/2)\rho g b l_{mo}^2$$

The moments are

$$\begin{aligned} M_D &= -F_D x_\eta = -K_D\left(\tau_o + \Delta\tau + \tau_o\frac{\Delta l}{l_{mo}}\right)(x_{\eta o} - \eta\Delta l) \\ &= -K_D\tau_o x_{\eta o} - K_D x_{\eta o}\Delta\tau - K_D\left(\frac{x_{\eta o}\tau_o}{l_{mo}} - \eta\tau_o\right)\Delta l \end{aligned} \qquad (5)$$

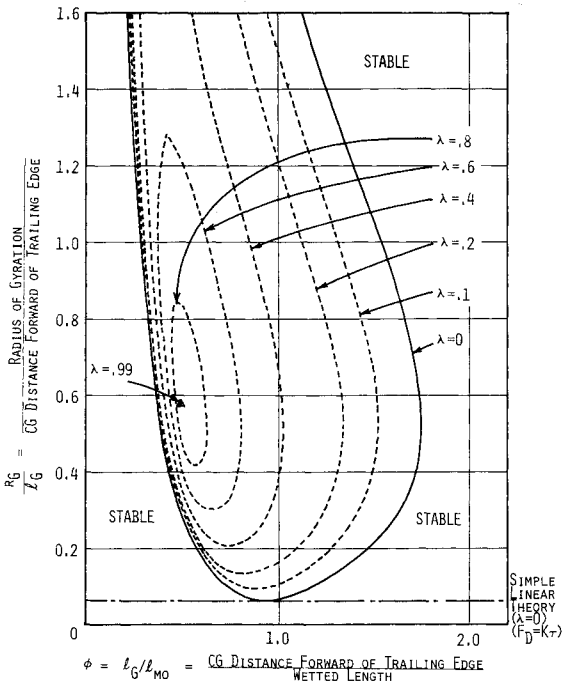

Fig. 2 Porpoising stability contours of Eq. (7), involving only "quasi-static" forces on a planing plate. λ = hydrostatic force/total normal force.

and

$$M_H = -F_H\left(x_H - \frac{1}{3}\Delta l\right)$$

$$= -K_H\tau_o x_H - K_H x_H \Delta\tau - 2K_H\tau_o \frac{x_H}{l_{mo}}\Delta l + \frac{K_H\tau_o}{3}\Delta l \quad (6)$$

Making these substitutions in the equations of motion, we get, since $\ddot{x}_m = -\ddot{l}$

$$\frac{W}{g}x_{mo}\ddot{\tau} - (K_D + K_H)\Delta\tau - \frac{W}{g}\tau_o\ddot{l} - (K_D\tau_o + 2K_H\tau_o)\frac{\Delta l}{l_{mo}} = 0$$

$$I\ddot{\tau} + (K_D x_{\eta o} + K_H x_H)\Delta\tau + \left[K_D\left(\frac{x_{\eta o}\tau_o}{l_{mo}} - \eta_D\tau_o\right) + K_H\tau_o\left(\frac{2x_H}{l_{mo}} - \frac{1}{3}\right)\right]\Delta l = 0$$

We define $\lambda = F_H/W = F_H/(F_H + F_D)$, the ratio of hydrostatic to total normal force and divide throughout by W to obtain

$$\left.\begin{aligned} &\frac{x_{mo}}{g}\ddot{\tau} - \frac{\Delta\tau}{\tau_o} - \frac{\tau_o}{g}\ddot{l} - (1+\lambda)\frac{\Delta l}{l_{mo}} = 0 \\ &\frac{r_G^2}{g}\ddot{\tau} + [(1-\lambda)x_{\eta o} + \lambda x_H]\frac{\Delta\tau}{\tau_o} + \left[(1-\lambda)\left(\frac{x_{\eta o}}{l_{mo}} - \eta_D\right) + \lambda\left(\frac{2x_H}{l_{mo}} - \frac{1}{3}\right)\right]\Delta l = 0 \end{aligned}\right\} \quad (7)$$

Writing these equations as

$$(a_1\ddot{\tau} + c_1\Delta\tau) + (a_2\ddot{l} + c_2\Delta l) = 0$$

$$(a_3\ddot{\tau} + c_3\Delta\tau) + c_4\Delta l = 0$$

we have

$$a_1 = \frac{x_{mo}}{g} = \frac{l_G}{g}\left(1 - \frac{1}{\phi}\right)$$

$$a_2 = -\frac{\tau_o}{g}$$

$$a_3 = \frac{r_G^2}{g}$$

$$c_1 = -\frac{1}{\tau_o}$$

$$c_2 = -\frac{\phi}{l_G}(1+\lambda)$$

$$c_3 = \frac{l_G}{\tau_o}\left[1 - \frac{\eta_D}{\phi} + \frac{\lambda}{\phi}\left(\eta_D - \frac{1}{3}\right)\right]$$

$$c_4 = (1-\lambda)(\phi - 2\eta_D) + \lambda(2\phi - 1)$$

The characteristic equation determinant is

$$\begin{vmatrix} (a_1\lambda^2 + c_1) & (a_2\lambda^2 + c_2) \\ (a_3\lambda^2 + c_3) & c_4 \end{vmatrix} = 0$$

which gives $A\lambda^4 + B\lambda^2 + C = 0$ (8)

where $A = a_2a_3 = \tau_o(r_G/g)^2$

$$B = a_2c_3 + a_3c_2 - a_1c_4$$

$$= \frac{l_G}{g}\left\{\phi(1+\lambda)\left[1 + \left(\frac{r_G}{l_G}\right)^2\right] - 2\eta(1-\lambda)\left(1 - \frac{1}{2\phi}\right) - 2\lambda\left(1 - \frac{1}{3\phi}\right)\right\} \quad (9)$$

$$C = c_2c_3 - c_1c_4 = \frac{1}{\tau_o}\left[\eta + \lambda(\lambda - 2)\left(\eta - \frac{1}{3}\right)\right] \quad (10)$$

It is interesting to note that the "static stability" coefficient C indicates that a planing surface is always statically stable so long as the center of pressure is forward of the trailing edge. This same result is obtained in more precise formulations of the problem, and may explain why a planing boat is so much easier to stabilize than an airfoil; or, for that matter, a submerged hydrofoil.

A plate which is free only in pitch will not be statically stable if the c.g. is behind the center of pressure (c.p.). It is the freedom in heave, itself highly stable, which couples with pitch to produce the unusual result of positive static stability for any c.g. location.

The familiar Routh's[4] discriminent can now be employed to study the stability boundaries of Eq. (8). In practice, it is quite unwieldy to write out for even this simplified quasi-static analysis, and it is better to evaluate it numerically.

The stability boundaries are presented in Fig. 2. The surface in ϕ, (r_G/l_G), λ space may be viewed as a mountain range, of local height λ. The range extends asymptotically to $r_G/l_G = \infty$. As $r_G/l_G \to \infty$ the thickness and height of the range tend to zero, and its location tends to $\phi = 0$. All combinations of r_G/l_G, ϕ and λ inside the range are unstable; all others are stable.

The peak of the mountain is a fine point, of altitude $\lambda = 1$, located at $r_G/l_G = 0.58$, $\phi = 0.5$.

For each value of λ there is a minimum critical value of r_g/l_G, below which the motion is stable for any c.g. position ϕ. It can be shown that this minimum value is what would be calculated if, instead of Eq. (1), we had assumed a simple linear dynamic lift relationship, $F_D = K\tau$. Thus, the terms accounting for the change in normal force and moment with wetted length l_m are clearly stabilizing. One is tempted to conclude that the region of instability can be further reduced by so shaping the planing surface that the changes in normal force and moment with l_m are enhanced; by the use of a triangular planform with the vertex aft, for example.

Since we have neglected any transient forces which may act on a disturbed planing plate, it is not to be expected

that Fig. 2 will agree quantitatively with what is observed in nature. But we should expect the general concept of stability depending on c.g. position ϕ and radius of gyration ratio r_G/l_G to be valid; especially the existence of low ϕ and high ϕ zones of stability, with an unstable zone in between. We might also expect the quantitative values to be valid when the frequency of the motion is very slow; when r_G/l_G is very large, for instance.

Transient Water Forces

To solve the general porpoising problem, we need to determine the transient water forces which act on a heaving, pitching plate. To accomplish this, we use the "virtual mass" slender body theory originally developed by Munk[5] and R. T. Jones,[6] and extended to oscillating wing theory by Ribner.[7] Although not as rigorous as general slender body theory, this approach has the advantage of permitting derivatives to be estimated rapidly, and the results generally agree with those obtained from a more rigorous analysis.

A pitch rate $\dot{\tau}$ and a heave velocity $\dot{y}$ will result in a total velocity normal to the planing surface of

$$v = u_o\tau + x\dot{\tau} - \dot{y} \tag{11}$$

If m' is the virtual water mass per unit length associated with the planing surface ($m' = \frac{1}{2}\rho\pi(b/2)^2 = \frac{1}{8}\rho\pi b^2$ for a flat plate[8]) the local transient force is given by

$$\frac{dF}{dx} = \frac{d}{dt}(m'v) = m'\frac{dv}{dt} + v\frac{dm'}{dt} \tag{12}$$

$dm'/dt = 0$ for a parallel sided plate, except in the discontinuity at $x = x_m$. Across this discontinuity

$$\Delta_1 F_T = v_m\int_{-\Delta t}^{+\Delta t}\frac{dm'}{dt}\,dt = v_m\int_{-\Delta t}^{+\Delta t}\frac{dm'}{dx}\frac{dx}{dt}\,dt$$

$$= u_o v_m\int_{-\Delta x}^{+\Delta x} dm' = u_o v_m m'$$

$$= u_o^2\tau m' + x_m u_o\dot{\tau}m' - u_o\dot{y}m' \tag{13}$$

The first term in Eq. (13) is the slender body version of the conventional planing lift, i.e.

$$F_{D_{SB}} = \frac{1}{2}\rho u_o^2\pi b^2\frac{\tau}{4} \tag{14}$$

This is identical with Eq. (1) when $l_m = b$. For a truly slender planing surface ($l_m/b \to \infty$), Shuford's equation gives a lift equal to twice the slender body value.¶ For a constant freestream velocity u_o, the first term in Eq. (12) gives the distributed force

$$\Delta_2 F_T = m'\int_{x_m}^{l_G}(u_o\dot{\tau} - \ddot{y} + x\ddot{\tau})dx$$

$$= m'\left[(u_o\dot{\tau} - \ddot{y})/l_G - x_m) + \frac{\ddot{\tau}}{2}(l_G^2 - x_m^2)\right] \tag{15}$$

Combining the transient terms of Eqs. (13) and (15)

$$\Delta F_T = m'\left[u_o l_G\dot{\tau} - l_{mo}\ddot{y} - u_o\dot{y} + l_m\left(l_G - \frac{1}{2}l_m\right)\ddot{\tau}\right]$$

The moment of the stagnation line forces about the c.g. is, from Eq. (13)

$$\Delta_1 M_T = m'u_o(x_m^2\dot{\tau} - x_m\dot{y}) \tag{17}$$

The distributed forces give a moment equal to

$$\Delta_2 M_T = -m'\int_{x_m}^{l_G}[(u_o\dot{\tau} - \ddot{y})x + x^2\ddot{\tau}]dx$$

$$= -m'\left[\frac{1}{2}(u_o\dot{\tau} - \ddot{y})(l_G^2 - x_m^2) + \frac{1}{3}(l_G^3 - x_m^3)\ddot{\tau}\right] \tag{18}$$

Combining the two

$$\Delta M_T = -m'\left[\frac{1}{2}u_o\dot{\tau}(l_G^2 + x_m^2) - \frac{1}{2}\ddot{y}(l_G^2 - x_m^2) + \frac{1}{3}\ddot{\tau}(l_G^3 - x_m^3)\right] \tag{19}$$

Substituting Eqs. (2) for $\dot{y}, \ddot{y}$, we finally obtain

$$\Delta F_T = m'l_{mo}\left[\frac{1}{2}l_{mo}\ddot{\tau} + u_o\dot{\tau} + \tau_o\ddot{l} + (u_o\tau_o/l_{mo})\dot{l}\right] \tag{20}$$

[Only the last term in $\dot{l}$ is contributed by the $\Delta_1 F_T$ force. The terms in τ- cancel out when Eq. (2) is substituted for $\ddot{y}$].

The transient moment becomes

$$\Delta M_T = -m'l_{mo}\left[\frac{1}{2}l_{mo}\left(l_G - \frac{1}{3}l_{mo}\right)\ddot{\tau} + \frac{u_o}{l_{mo}}\left(l_G^2 - l_G l_m + \frac{1}{2}l_m^2\right)\dot{\tau} + \tau_o\left(l_G - \frac{1}{2}l_{mo}\right)\ddot{l}\right] \tag{21}$$

In this equation, the $\Delta_1 F_T$ force contributes a small term $m'u_o(l_G - l_m)^2\dot{\tau}$ to the pitch damping.

With the nondimensionalizing scheme employed in this paper, it is convenient to define a ratio

$$\gamma = \frac{gm'l_{mo}}{W} = \frac{\text{weight of virtual mass of water}}{\text{weight supported by the plate}}$$

The transient force and moment terms can then be written as

$$\Delta F_T = W\frac{\gamma}{g}\left[\frac{1}{2}l_{mo}\ddot{\tau} + u_o\dot{\tau} + \tau_o\ddot{l} + \frac{u_o\tau_o}{l_{mo}}\dot{l}\right] \tag{22}$$

$$\Delta M_T = -W\gamma\frac{l_G}{g}\left\{\frac{1}{2}l_G\left[\frac{1}{\phi} - \left(\frac{1}{3\phi}\right)^2\right]\ddot{\tau} + u_o\phi\left[1 - \frac{1}{\phi} + \left(\frac{1}{2\phi}\right)^2\right]\dot{\tau} + \tau_o\left(1 - \frac{1}{2\phi}\right)\ddot{l}\right\} \tag{23}$$

Before proceeding to substitute these transient terms into the equations of motion, it is of interest to identify some of them more explicitly. The terms

$$-(m'l_{mo})\ddot{y} + (m'l_{mo})\left(l_G - \frac{1}{2}l_{mo}\right)\ddot{\tau} \quad \text{in Eq. (16)}$$

and

$$+\frac{1}{2}m'(l_G^2 - x_m^2)\ddot{y} - \frac{1}{3}m'(l_G^3 - x_m^3)\ddot{\tau} \quad \text{in Eq. (19)}$$

represent the reactance of the water mass $m'l_{mo}$ to vertical and angular acceleration.

The components of Eqs. (16) and (19) are presented in Table 1 in a form similar to that employed in aircraft stability analysis, and compared with Ribner's results for triangular wings. Apart from differences attributable to the different planforms, and the fact that the "virtual mass" of a planing plate is half that of a wing, the correspondence is clearly good.

Complete Equations of Motion

Combining Eqs. (7, 22, and 23), we obtain

$$\frac{l_G}{g}\left(1 - \frac{1}{\phi} - \frac{\gamma}{2\phi}\right)\ddot{\tau} - \frac{\gamma u_o}{g}\dot{\tau} - \frac{\Delta\tau}{\tau_o} - \frac{\tau_o}{g}(1+\gamma)\ddot{l} - \frac{\gamma}{g}\frac{u_o\tau_o}{l_{mo}}\dot{l} - (1+\lambda)\frac{\Delta l}{l_{mo}} = 0$$

¶An anomoly which also occurs in airfoil theory.

Table 1 Comparison of planning surface derivatives with the corresponding values for slender wings

	For a Planing Plate		
	Stagnation line component	Distributed component	From triangular slender wing theory of Ribner[7]
Normal force coefficient $C_{N\tau} = F_N \Big/ \frac{1}{2}\rho u_o^2 S\tau$	$\frac{\pi}{4}A$	—	$\frac{\pi}{2}A$
Pitch rate derivative $C_{N\dot{\tau}}$	$\frac{\pi}{4}(\phi - 1)$	$\frac{\pi}{4}$	$\frac{\pi}{2}\phi$
Pitch accelerative derivative $C_{N\ddot{\tau}}$	—	$\frac{\pi}{4}A\left(\phi - \frac{1}{2}\right)$	$\frac{\pi}{2}A\left(\frac{\phi}{3} - \frac{1}{12}\right)$
Heave velocity derivative $C_{N\dot{y}}$	$-\frac{\pi}{4}A$	—	$-\frac{\pi}{2}A$
Heave acceleration derivative $C_{N\ddot{y}}$	—	$-\frac{\pi}{4}$	$-\frac{\pi}{6}$
Moment coefficient $C_m = M \Big/ \frac{1}{2}\rho u_o^2 S b\tau$	$-\frac{\pi}{4}(\phi - 1)$	—	$-\frac{\pi}{2}\left(\phi - \frac{1}{3}\right)$
Pitch rate derivative $C_{m\dot{\tau}}$	$-\frac{\pi}{4A}(\phi - 1)^2$	$-\frac{\pi}{4A}\left(\phi - \frac{1}{2}\right)$	$-\frac{\pi}{2A}\left(\phi^2 - \frac{1}{3}\phi + \frac{1}{12}\right)$
Pitch acceleration derivative $C_{m\ddot{\tau}}$	—	$-\frac{\pi}{4}A^2\left(\phi^2 - \phi - \frac{1}{3}\right)$	$-\frac{\pi}{6A^2}\left(\phi^2 - \frac{1}{2}\phi + \frac{1}{10}\right)$
Heave velocity derivative $C_{m\dot{y}}$	$\frac{\pi}{4}(\phi - 1)$	—	$\frac{\pi}{2}\left(\phi - \frac{1}{3}\right)$
Heave acceleration derivative $C_{m\ddot{y}}$	—	$\frac{\pi}{4A}\left(\phi - \frac{1}{2}\right)$	$\frac{\pi}{6A}\left(\phi - \frac{1}{4}\right)$

The nondimensional parameters in these relationships are τ, $b\dot{\tau}/u_o$, $b\ddot{\tau}^2/u_o^2$, $\dot{y}/u_o$, $b\ddot{y}/u_o^2$.

$$\frac{l_G^2}{g}\left[\left(\frac{r_G}{l_G}\right)^2 + \frac{\gamma}{2\phi}\left(1 - \frac{1}{3\phi}\right)\right]\ddot{\tau} + \frac{l_G}{g}\gamma u_o\left(\phi - 1 + \frac{1}{2\phi}\right)\dot{\tau} + \frac{l_G}{\tau_o}\left[1 - \frac{\eta_D}{\phi} + \frac{\lambda}{\phi}\left(\eta_D - \frac{1}{3}\right)\right]\Delta\tau \quad (24)$$

$$+ \gamma\frac{l_G}{g}\tau_o\left(1 - \frac{1}{2\phi}\right)\ddot{l} + [\,(1-\lambda)(\phi - 2\eta_D) + \lambda(2\phi - 1)\,]\Delta l = 0$$

We now express the equations in terms of nondimensional parameters. Let

$$R = \frac{r_G}{l_G}$$

$$\hat{l} = \frac{\Delta l}{l_{mo}}$$

$$\hat{\tau} = \frac{\Delta\tau}{\tau_o}$$

$$\hat{t} = \frac{u_o}{l_{mo}}t$$

$$f = F^2\tau_o = \frac{u_o^2}{g l_{mo}}\tau_o$$

Note that f is a kind of loading parameter, i.e.

$$f = \tau_o F^2 = \frac{W}{\frac{1}{2}\rho g\pi b^2 l_{mo} C_\tau} = \frac{W}{4M'C_\tau} = \frac{1}{4\gamma C_\tau}$$

where M' is the *total* associated virtual mass $1/8\rho g\pi b^2 l_{mo} = m' l_{mo}$, and $F = u_o/(g l_{mo})^{1/2}$ is the Froude number.

Also let a dash ($\hat{\tau}$) denote differentiation with respect to $\hat{t}$. Then

$$\dot{\tau} = \frac{u_o}{l_{mo}}\tau' \qquad \ddot{\tau} = \frac{u_o^2}{l_{mo}^2}\hat{\tau}''$$

$$\dot{l} = u_o\hat{l}' \qquad \ddot{l} = \frac{u_o^2}{l_{mo}}\hat{l}''$$

The equations then become

$$\left.\begin{aligned} a_1\hat{\tau}'' + b_1\hat{\tau}' + c_1 + a_2\hat{l}'' + b_2\hat{l}' + c_2 = 0 \\ a_3\hat{\tau}'' + b_3\hat{\tau}' + c_3 + a_4\hat{l}'' + b_4\hat{l}' + c_4 = 0 \end{aligned}\right\} \quad (25)$$

where

$$a_1 = f\left(\phi - 1 - \frac{\gamma}{2}\right) \qquad b_1 = -f\gamma$$

$$a_2 = -f(1+\gamma) \qquad b_2 = -f\gamma$$

$$a_3 = f\left[\phi R^2 + \frac{\gamma}{2}\left(1 - \frac{1}{3\phi}\right)\right] \qquad b_3 = f\gamma\left(\phi - 1 + \frac{1}{2\phi}\right)$$

$$a_4 = f\gamma\left(1 - \frac{1}{2\phi}\right) \qquad b_4 = 0$$

$$c_1 = -1$$

$$c_2 = -(1+\lambda)$$

$$c_3 = 1 - \frac{\eta_D}{\phi} + \frac{\lambda}{\phi}\left(\eta_D - \frac{1}{3}\right)$$

$$c_4 = (1-\lambda)\left(1 - \frac{2\eta_D}{\phi}\right) + \lambda\left(2 - \frac{1}{\phi}\right)$$

The corresponding characteristic equation is

$$A\lambda^4 + B\lambda^3 + C\lambda^2 + D\lambda + E = 0 \quad (26)$$

where

$$A = a_1a_4 - a_2a_3$$

$$B = a_4b_1 - a_2b_3 - a_3b_2$$

$$C = a_1c_4 + a_4c_1 - a_2c_3 - b_2b_3 - a_3c_2$$

$$D = b_1c_4 - b_2c_3 - b_3c_2$$

$$E = c_1c_4 - c_2c_3$$

The parameters

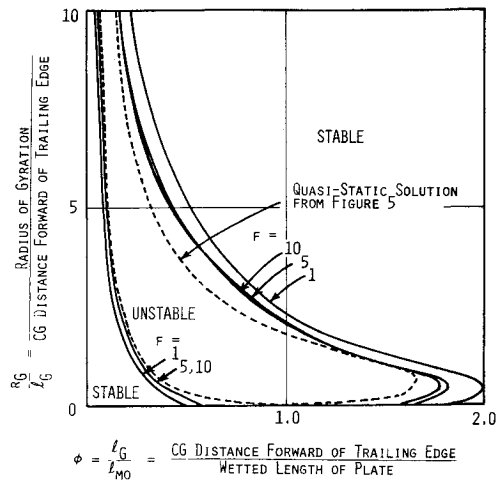

Fig. 3 Typical stability limits for very large values of the pitch inertia parameter r_G/l_G, $\lambda = 0$, $b/l_m = 0.1, 0.5$.

$$\gamma = \frac{(1 + b/l_{mo})}{2f} \tag{27}$$

and

$$\lambda = \frac{1}{1 + \{(\pi/2)F^2/[(1 + l_{mo})/b]\}} = \frac{1}{1 + \{\pi f/2[(1 + l_{mo})/b]\tau_o\}} \tag{28}$$

The static stability coefficient E in Eq. (26) is identical with Eq. (10). The other coefficients, A–D, are given by quite lengthy expressions, and will not be reproduced here.

The stability limits of Eqs. (25) are plotted for some typical cases in Figs. 3–11. Characteristically, there is a stable zone when the c.g. is close to the transom. This would require a substantial nose down moment to trim, such as would be experienced in the case of an "airboat." It is also the region we might expect a flying boat or seaplane to operate in at the beginning of its takeoff run.

The second stable zone occurs when the c.g. is forward of the stagnation region, which is often the case for slender high-speed boats. The normal rule of thumb is to move the c.g. forward if a boat porpoises, and Figs. 3–11 show clearly why this is so for many cases. But in marginal cases, moving the c.g. forward by adding weight to the bow may be ineffective, because the favorable increase in ϕ is offset by an unfavorable increase in r_G.

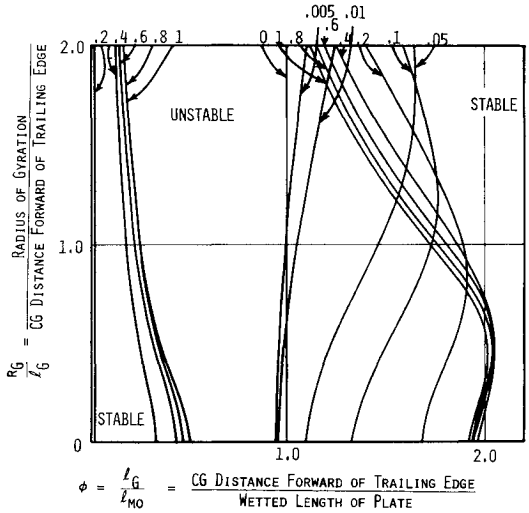

Fig. 4 Stability boundaries for $\lambda = 0$, $b/l_m = 0.1$. (The numbers on the curves give the value of the loading parameter $f = \tau_o F^2$.)

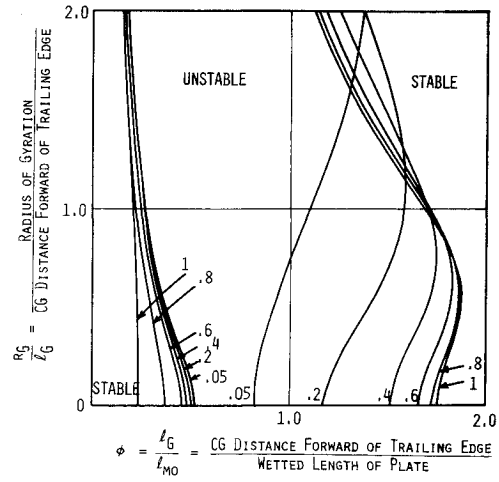

Fig. 5 Stability boundaries for $\lambda = 0$, $b/l_m = 0.5$. (The numbers on the curves give the value of the loading parameter $f = \tau_o F^2$.)

In Fig. 3, we show the stability boundaries for very large values of the pitch inertia parameter r_G/l_G. They are quite insensitive to variations in both f and b/l_m, and follow very closely the corresponding "quasi-static" stability boundaries of Fig. 2. It thus appears that the transient water force terms are not important in this case; a discovery which is not particularly surprising.

Figures 4–7 show the boundaries for $\lambda = 0$ (zero buoyant contribution) for various aspect ratios, b/l_{mo} for a range of r_G/l_G more appropriate to current practice. The slender planing surfaces have a quite large unstable range, even down to zero pitch inertia. At and above $b/l_{mo} = 1.0$ (Fig. 6) however, the unstable region vanishes for low values of f. A combination of high-aspect ratio and reasonably low f can avoid instability altogether. Above $b/l_{mo} \simeq 4$ or 5, no instability can be detected at all.

Corresponding plots with the buoyancy parameter $\lambda = 0.4$ are given in Figs. 8–10. The trends are the same, but for each value of b/l_{mo} the unstable zone is reduced as λ is increased.

The concept of obtaining longitudinal stability by placing the c.g. forward of the center of pressure (c.p.) or more precisely, the aerodynamic center (a.c.) is one which is familiar from aircraft stability theory. Thus the c.g. forward region of stable planing is to be expected.

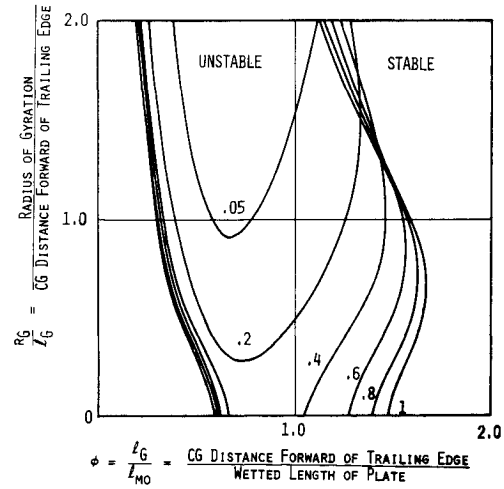

Fig. 6 Stability boundaries for $\lambda = 0$, $b/l_{mo} = 1.0$. (The numbers on the curves give the value of the loading parameter $f = \tau F^2$.)

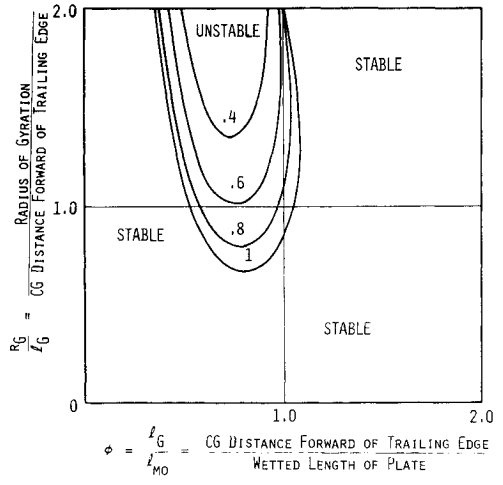

Fig. 7 Stability boundaries for $\lambda = 0$, $b/l_{mo} = 3.0$. (The numbers on the curves give the value of the loading parameter $f = \tau_o F^2$.)

The stable region predicted at low values of ϕ is without parallel in the aircraft case. It is presumably connected with the fact that a planing plate is statically stable with the c.g. behind the c.p. (due to the heave mode) because of the presence of the free surface.

It is interesting to note from Fig. 18 that the region of instability is reduced when the c.p. is further aft in relation to the wetted length. That is, when η_D is reduced below the value of 7/8 assumed for most of the charts.

Figures 7 and 11 particularly illustrate that a relatively high-aspect ratio ($A = 2$ or 3) planing surface can be stable for all values of ϕ, so long as the moment of inertia is below a critical value. This is certainly observed in practice with beamy flat or shallow-V bottomed "drag" and "ski" boats which in calm water plane on the last few inches of their bottoms, and can reach speeds of the order of 200 mph.

The uncoupled equations for heave and pitch are of some interest, and expressed in terms of real time, they are

$$(1+\gamma)\ddot{y} + \frac{\gamma u_o}{l_{mo}} y + (1+\lambda)\frac{g}{l_{mo}}\Delta y = 0 \tag{29}$$

$$\left[\left(\frac{r_G}{l_G}\right)^2 + \frac{\gamma}{2\phi}\left(1 - \frac{1}{3\phi}\right)\right]\ddot{\tau} + \left(\phi - 1 + \frac{1}{2\phi}\right)\gamma\frac{u_o}{l_{mo}}\dot{\tau} + \frac{g}{l_G}\left[1 - \frac{\eta_D}{\phi} + \frac{\lambda}{\phi}\left(\eta_D - \frac{1}{3}\right)\right]\Delta\tau = 0 \tag{30}$$

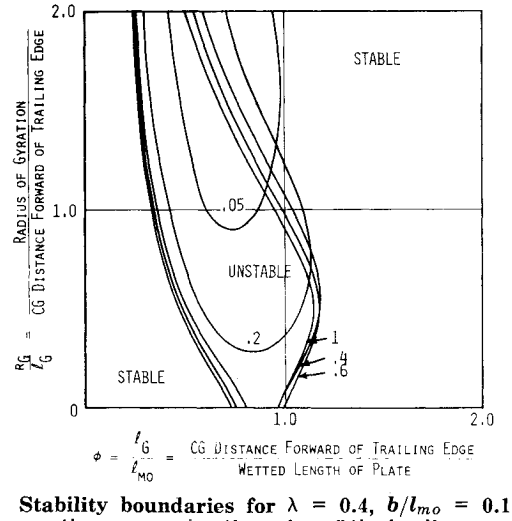

Fig. 8 Stability boundaries for $\lambda = 0.4$, $b/l_{mo} = 0.1$. (The numbers on the curves give the value of the loading parameter $f = \tau_o F^2$.)

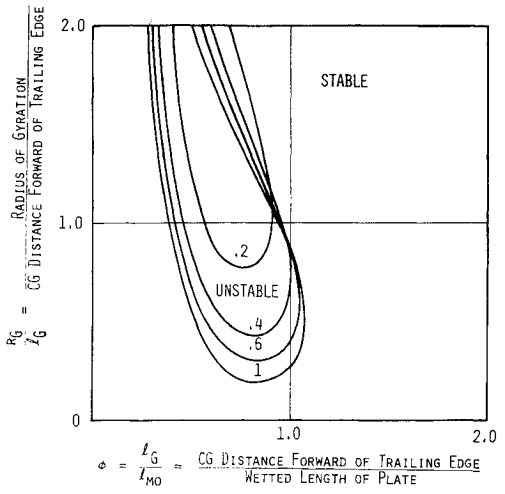

Fig. 9 Stability boundaries for $\lambda = 0.4$, $b/l_{mo} = 0.5$. (The numbers on the curves give the value of the loading parameter $f = \tau_o F^2$.)

The uncoupled natural frequencies and critical damping coefficient ratios are therefore

Heave

$$\omega_H = \frac{u_o}{l_m} \cdot \frac{1}{F}\left(\frac{1+\lambda}{1+\gamma}\right)^{1/2} \tag{31}$$

$$\bar{C}_H = \frac{C}{\omega} = \frac{\gamma}{2}F\left(\frac{1+\gamma}{1+\lambda}\right)^{1/2} \tag{32}$$

Pitch

$$\omega_P = \frac{u_o}{l_m} \cdot \frac{1}{F}\left\{\frac{\left[1 - \frac{\eta_D}{\phi} + \frac{\lambda}{\phi}\left(\eta_D - \frac{1}{3}\right)\right]}{\left[\phi\left(\frac{r_G}{l_G}\right)^2 + \frac{\gamma}{2}\left(1 - \frac{1}{3\phi}\right)\right]}\right\}^{1/2} \tag{33}$$

$$\bar{C}_P = \frac{\gamma}{2}F\left(\phi - 1 + \frac{1}{2\phi}\right)\left\{\frac{\left[\phi\left(\frac{r_G}{l_G}\right)^2 + \frac{\gamma}{2}\left(1 - \frac{1}{3\phi}\right)\right]}{\left[1 - \frac{\eta_D}{\phi} + \frac{\lambda}{\phi}\left(\eta_D - \frac{1}{3}\right)\right]}\right\}^{1/2} \tag{34}$$

From Eqs. (31) and (32), it is obvious that heave frequency and damping are always positive and finite. From Eq. (30) it is clear that pitch stiffness becomes negative when

$$\phi < \eta_D - \lambda\left(\eta_D - \frac{1}{3}\right)^{**}$$

Pitch damping is always positive. The minimum value occurs when $\phi = 1/(\sqrt{2})^{1/2}$.

Effect of Deadrise Angle

The foregoing analysis has been carried out for a flat plate planing surface. When the planing surface is prismatic, of deadrise angle β, both the steady-state lift and the virtual mass are reduced. Shuford[3] uses an empirical factor of

$$\psi = \frac{C_\tau}{\text{Flat Plate } C_\tau} = (1 - \sin\beta) \tag{35}$$

to attenuate Eq. (1).

The variation of the virtual mass coefficient with β for a rhomboid[9] is compared with Eq. (35) in Fig. 12, together with Wagner's[10] iterative approximation. It is not clear that the rhomboid is strictly analogous to a planing wedge however, because the latter does not experience in-

**When ϕ is less than this value, the motion is statically stabilized by heave motion. Without this freedom in heave, Eq. (34) shows that many boats would be statically unstable at high speeds.

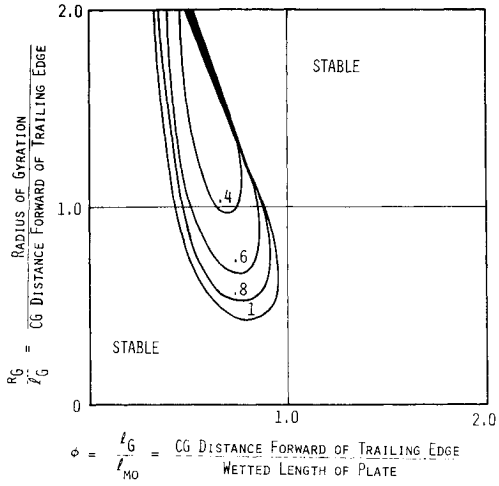

Fig. 10 Stability boundaries for $\lambda = 0.4$, $b/l_{mo} = 1.0$. (The numbers on the curves give the value of the loading parameter $f = \tau_o F^2$.)

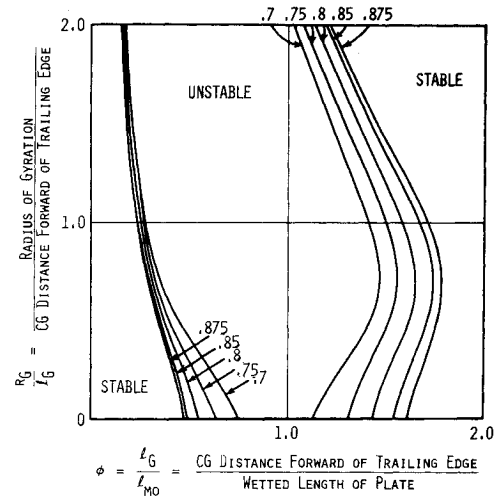

Fig. 11 The effect of varying the dynamic center of pressure parameter η_D on the stability boundaries for a typical case. $\lambda = 0$, $b/l_{mo} = 0.5$, $f = F^2\tau_o = 0.5$. (The numbers on the curves give the assumed center of pressure position as a fraction of l_m.)

finite water velocity at the chines. Additionally, there is some experimental evidence[11] that the Wagner-Von Kármán theories of wedge impact over estimate actual values.

Because of this, we have elected to use Eq. (35) as an attenuator for the virtual mass terms, as well as the steady-state lift curve slope C_τ.

The corresponding coefficients for Eq. (25) are then as follows:

For $\lambda = 0$

$$\left.\begin{aligned} a_1 &= f(\phi - 1 - \frac{\gamma}{2}\psi) & b_1 &= -f\gamma\psi \\ a_2 &= -f(1 + \gamma\psi) & b_2 &= -f\gamma\psi \\ a_3 &= f\left[\phi R^2 + \frac{\gamma\psi}{2}\left(1 - \frac{1}{3\phi}\right)\right] & b_3 &= f\gamma\psi\left(\phi - 1 + \frac{1}{2\phi}\right) \\ a_4 &= f\gamma\psi\left(1 - \frac{1}{2\phi}\right) & b_4 &= 0 \\ & & c_1 &= -\psi \\ & & c_2 &= -\psi \\ & & c_3 &= \psi(1 - \frac{\eta_D}{\phi}) \\ & & c_4 &= \psi(1 - \frac{2\eta_D}{\phi}) \end{aligned}\right\} \quad (36)$$

An example of the resulting stability boundaries is given in Fig. 13. The effect of ψ is seen to be quite small, partially justifying the rather crude characterization of ψ employed in the analysis.

Laplace Transform of the Equations of Motion

If $\bar{\tau}$ and $\bar{l}$ are the Laplace transforms of $\hat{\tau}$ and $\hat{l}$, and if $\hat{\tau}_o$ is an initial angular disturbance velocity value, then Eq. (25) can be written as

$$\left.\begin{aligned} (a_1 s^2 + b_1 s + c_1)\bar{\tau} + (a_2 s^2 + b_2 s + c_2)\bar{l} &= \tau_o' \\ (a_3 s^2 + b_3 s + c_3)\bar{\tau} + (a_4 s^2 + c_4)\bar{l} &= \tau_o' \end{aligned}\right\} \quad (37)$$

Eliminating $\bar{l}$

$$\left\{\frac{[1]}{[2]} - \frac{[3]}{[4]}\right\}\bar{\tau} = \left\{\frac{1}{[2]} - \frac{1}{[4]}\right\}\tau_o'$$

Multiplying both sides by [2][4]

$$\{[1][4] - [2][3]\}\bar{\tau} = \{[4] - [2]\}\tau_o'$$

It may easily be verified that the left hand side is a quartic in s with the same coefficients as Eq. (26), the characteristic equation.

Thus

$$\left.\begin{aligned} \frac{\bar{\tau}}{\tau_o'} &= \frac{(a_4 - a_2)s^2 - b_2 s + (c_4 - c_2)}{As^4 + Bs^3 + Cs^2 + Ds + E} \\ \frac{\bar{l}}{\tau_o'} &= \frac{(a_3 - a_1)s^2 + (b_3 - b_1)s + (c_3 - c_1)}{As^4 + Bs^3 + Cs^2 + Ds + E} \end{aligned}\right\} \quad (38)$$

Expressed in this way, the variation of τ and l with time is readily obtained using one of the Laplace inversion routines found in most computer libraries. Examples of such solutions for the low ϕ and high ϕ stable regions are given in Figs. 14 and 15. The corresponding motion in the intermediate unstable region is given in Fig. 16.

The frequency of the oscillation is given by $n/2\pi$ Hertz, where n is the complex portion of the conjugate complex roots of the characteristic equation, $As^4 + \ldots E = 0$.

For the cases illustrated in Figs. 14–16, namely

$\lambda = 0$, $f = 0.5$, $b/l_{mo} = 0.5$, $r_G/l_G = 1.6$

we have	Rear Stable Region	Forward Stable Region	Unstable Region
$\phi =$	0.1	2.0	1.0
First root pair	$-1.7307 \pm 0.61854i$	$-0.20197 \pm 0.36438i$	$-0.53901 \pm 0.61337i$
Second root pair	$-0.06446 \pm 1.2948i$	$-0.19470 \pm 0.80660i$	$+0.16229 \pm 0.84517i$
First $\frac{\omega}{2\pi}\frac{l_{mo}}{u_o}$	0.0984	0.0580	0.0975
Second $\frac{\omega}{2\pi}\frac{l_{mo}}{u_o}$	0.206	0.1283	0.1343

The motion thus consists of two sinusoidal oscillations corresponding to the two pairs of complex conjugate roots. The $\phi = 0.1$ has one highly damped and one lightly damped.

Stability and Static Trim

We have seen that for a slender planing surface at high speeds, the c.g. location parameter ϕ must either be quite small (c.g. close to the transom) or considerably greater than unity.

For roughly square planing surfaces alternatively, we can obtain stability by combination of a low moment of inertia and a low value of

$$f = \frac{W}{(1/2)\rho g \pi b^2 l_m C_\tau}$$

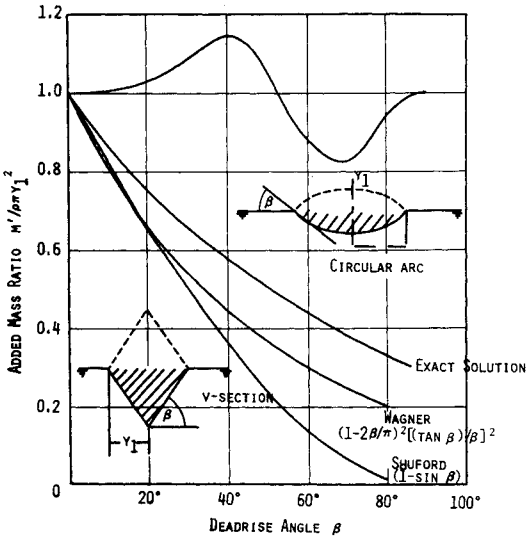

Fig. 12 Added mass ratios, in an infinite fluid, for rhombic and circular arc cylinders, as a function of "deadrise angle" at the SWL.

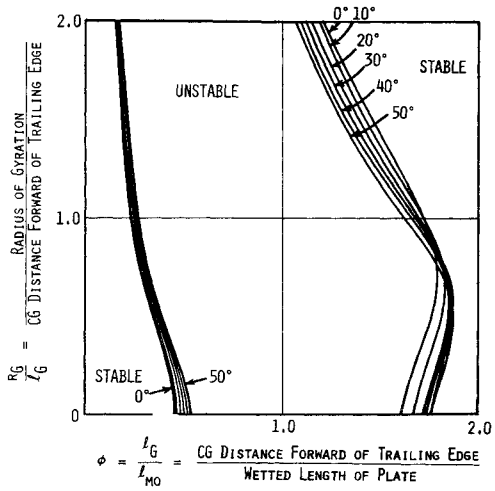

Fig. 13 The effect of deadrise angle upon the stability limits for a typical case. $\lambda = 0$, $b/l_{mo} = 0.5$, $f = F^2\tau_o = 0.5$.

That is, a light, beamy boat with a high dynamic lift curve slope C_T.

The simple trim geometry of a slender planing surface is depicted in Fig. 17 for the ideal case of either zero skin friction, or when skin friction has no net moment about the c.g. In this case, the "c.g. forward" case is considered for stabilization, and the balance of moments gives

$$F_N(l_G - \eta l_m) = T(h_G + p_1) - Ti(l_G + p_2)$$

Writing $T = W/(L/D)$, where L/D is the lift/drag ratio, the c.g. position for trim is given by

$$\phi = \frac{\eta}{1 - \left(\frac{D}{L}\right)\left[\left(\frac{h_G + p_1}{l_G}\right) - \left(1 + \frac{p_2}{l_G}\right)i\right]}$$

This expression is plotted in Fig. 18 for a practical range of h_G and propeller thrust axis inclination i. It should be noted that skin friction will generally contribute a nose down moment, so that achievable values of ϕ will be even lower than those given in Fig. 18.

The lift/drag ratio for conventional planing boats is in the range of 1 to 3, so that as indicated in Fig. 18, it is not too hard to trim for the ϕ values well in excess of unity which are required for conventional values of r_G/l_G. With increasing hull efficiency, it becomes progressively harder to balance the boat with the c.g. far enough forward to avoid porpoising.

For efficient, low drag hulls, there now seems to be four approaches to curing porpoising instability:

a) Introduce a large *down*-load at the stern (by excessive negative propeller inclination, a negatively set hydrofoil, etc.) to permit the c.g. to be moved far enough forward for stability. This is clearly undesirable, since it reduces the efficiency of the hull, but is widely employed with outboard and out-drive powered boats.
b) Move the c.g. aft into the "ϕ rearward" stability zone, and trim by a large *up*-load at the stern.
c) Introduce additional damping into the pitch and/or heave damping modes. This may be done synthetically (servo-operated trim tabs, for example), by configuration innovations such as spray rails or deflectors, or by changing the planform of the planing surface.

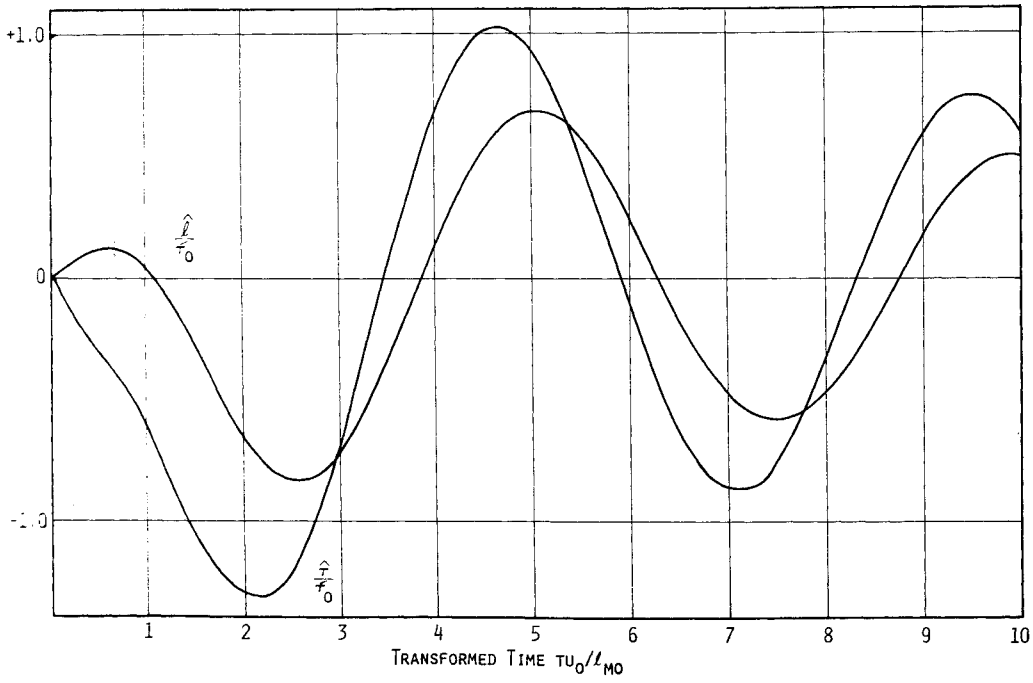

Fig. 14 Motion after an angular velocity disturbance $\hat{\tau}_o$ when the c.g. is in the "c.g. aft" region of stability. $\phi = 0.1$, $\lambda = 0$, $f = 0.5$, $b/l_{mo} = 0.5$, $r_G/l_{mo} = 1.6$.

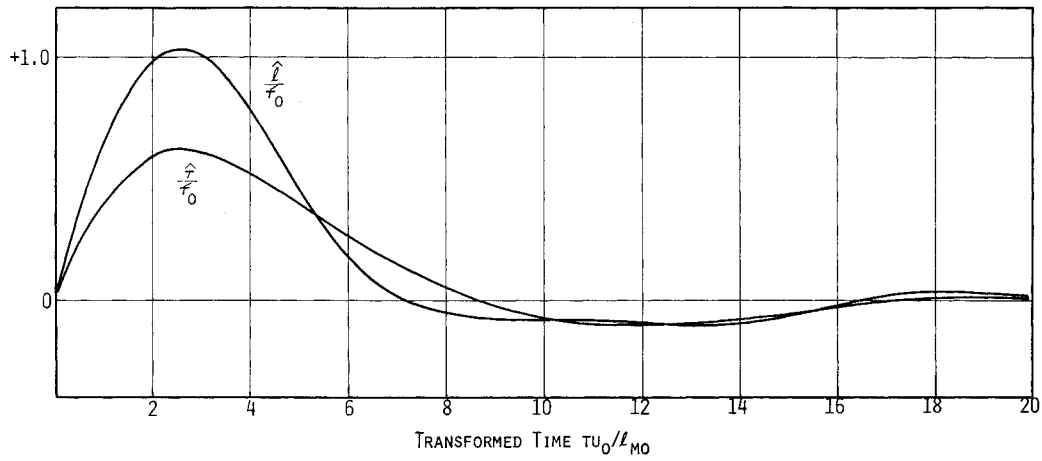

Fig. 15 Motion after an angular velocity disturbance $\dot{\tau}_0$ when the c.g. is in the "c.g. forward" region of stability. $\phi = 2.0$, $\lambda = 0$, $f = 0.5$, $b/l_{mo} = 0.5$, $r_G/l_{mo} = 1.6$.

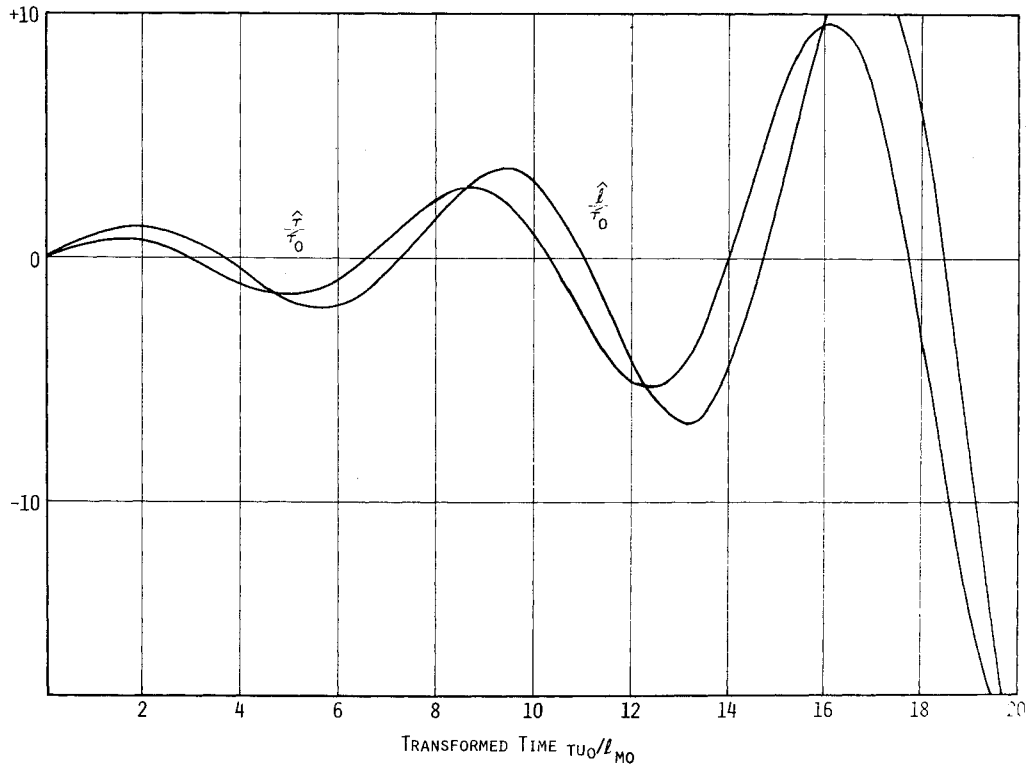

Fig. 16 Motion after an angular velocity disturbance $\dot{\tau}_0$ when the c.g. is in the unstable region. $\phi = 1.0$, $f = 0.5$, $b/l_m = 0.5$, $r_G/l_{mo} = 1.6$.

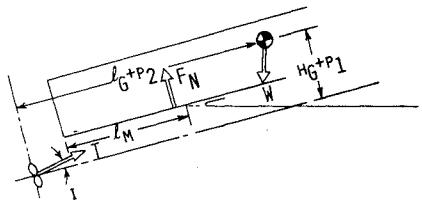

Fig. 17 Geometry for simple static trim balance.

d) Make the moment of inertia very large, so that r_G/l_G exceeds 2.5–3.0. Then, as shown by Fig. 3, the craft will be stable with the c.g. over the center of pressure.

The second solution is apparently used successfully on many racing hydroplanes, of which the Mollanari "tunnel hull" catamaran is perhaps the best known. The large upload at the stern is provided by a "hook" in the planing surface,†† equivalent to positive camber near the trailing edge. The disadvantage of this solution is that, with the c.g. well aft, the craft is very susceptible to *aerodynamic* pitch divergence; a phenomenon known as "flipping."

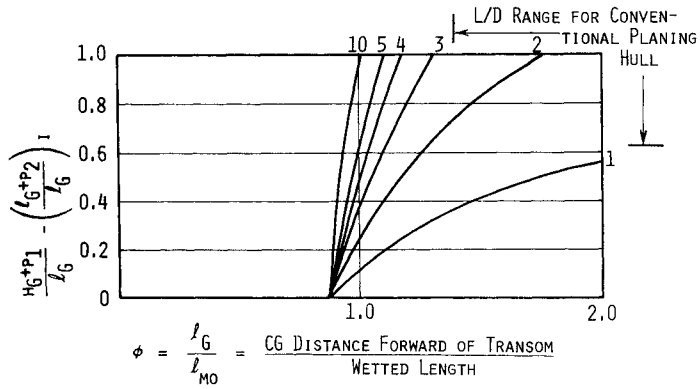

Fig. 18 c.g. position for trim, as a function of propeller location and thrust line angle i, neglecting skin friction moments.

††See Appendix I.

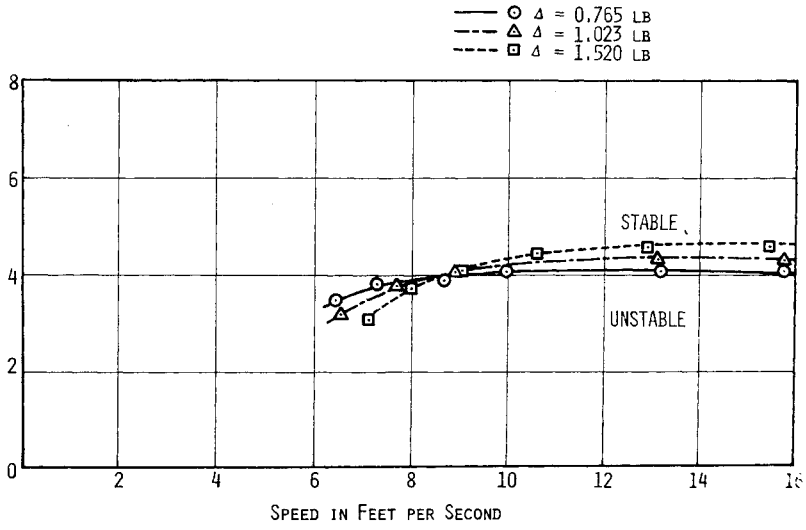

Fig. 19 Day and Haag[12] data for 2° oscillation porpoising limit on c.g. as a function of speed; for a flat planing surface.

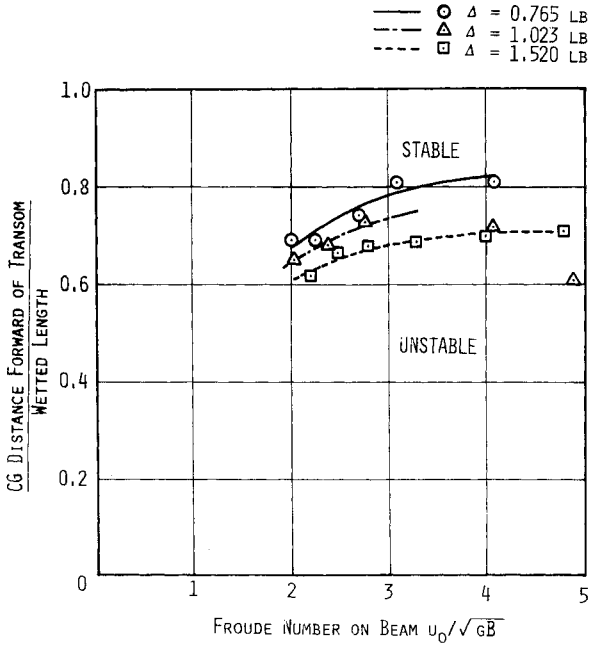

Fig. 20 The raw data of Day and Haag[12] as a function of Froude number.

Comparison with Experiment

Porpoising stability limits have been established in model basin experiments for a great many flying boat hulls, or hull and aerodynamic surface combinations, but the hull forms are too complex to permit comparison with the simple theory of this paper. In particular, they are susceptible to "high-trim porpoising" in which the afterbody is involved. A few reports on the porpoising of flat plate planing surfaces have been published, but only in the work of Day and Haag[12] is sufficient detail found‡‡ (particularly with regard to c.g. location and radius of gyration) to permit a comparison to be made with theory.

Exact agreement cannot be expected for four reasons:

1) Day and Haag define porpoising as trim oscillation of ±2° or greater.
2) The towing bridle was attached at a height up to one quarter of the beam above the c.g. The horizontal mismatch was even greater. Thus towing bridle forces will modify the equations of motion.
3) The mechanical system employed to record trim and heave motion introduces an unknown quantity of friction damping. The presence of this damping presumably explains why their porpoising was amplitude limited at a given value of $\pm\tau$ for a given c.g. position.
4) The "wetted length" was estimated by eye from the side of the tank.

The Day and Haag tests involved, essentially, varying the c.g. region, and plotted for each of Day and Haag's points, taking their quoted values of trim, wetted length, and so on, at face value, rather than attempting to smooth the

If one were unaware of the previous literature, one would be tempted to conclude from Fig. 19 that the model is unstable when the c.g. is aft of 4.0 in., and that an increased buoyancy contribution (greater weight at a given speed, or less speed) increases the stable range somewhat. One would then present the data as in Fig. 20, suspecting that the trends were all quite regular, and that the two highest speed points for Δ = 1.023 lb were somewhat in error.

If we plot the measured "wetted length" as in Fig. 28, we see that there is indeed something strange about the last two Δ = 1.023 lb points. Since one sees a progressive variation of the other two measured parameters (Figs. 19 and 22) it is presumably the wetted length measurements —the most difficult to make—which are in error.

In Figs. 23–25, the real part of the characteristic equation has been evaluated from the theory, in the unstable c.g. region, and plotted for each of Day and Haag's points, taking their quoted values of trim, wetted length, and so on, at face value, rather than attempting to smooth the data. The greater the value of the real part of the root, of course, the greater the instability. Superimposing their ±2° porpoising boundaries (as solid dots), it can be seen that they fall in the region of theoretical instability, but that otherwise no discernible trend is obvious. This is probably all that can be expected, under the circumstances.

The effect of 20% variations in trim and wetted length, on both the apparent observed ±2° boundary and the calculated unstable region is given in Fig. 26.

In any future measurements of porpoising stability, it might be as well to arrange for the model to be excited mechanically, as in aerodynamic flutter testing, and to search for the point where the damping becomes negative. Additionally, of course, the model should be propelled at the c.g., and no mechanical friction or damping should be permitted to be present.

‡‡Other investigators *assume* that c.g. location and radius of gyration are unimportant, and therefore not worth reporting.

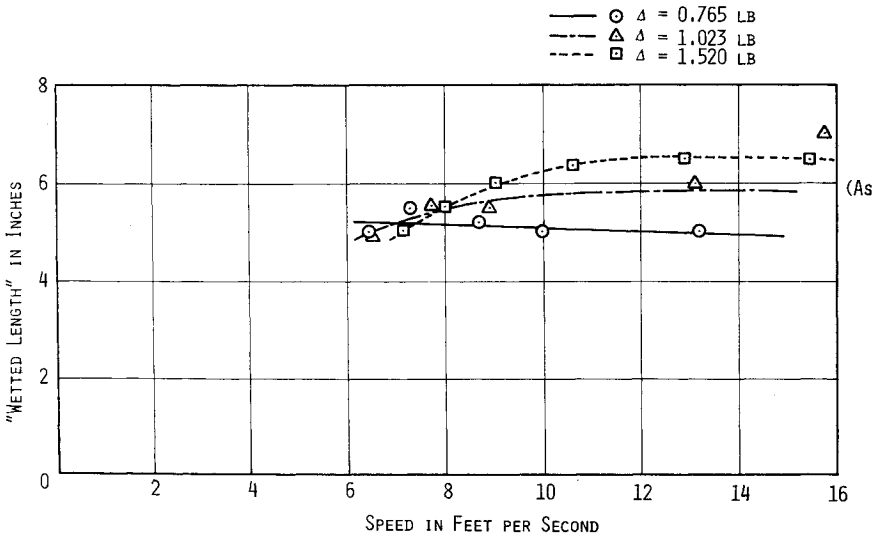

Fig. 21 Wetted length measured by Day and Haag.

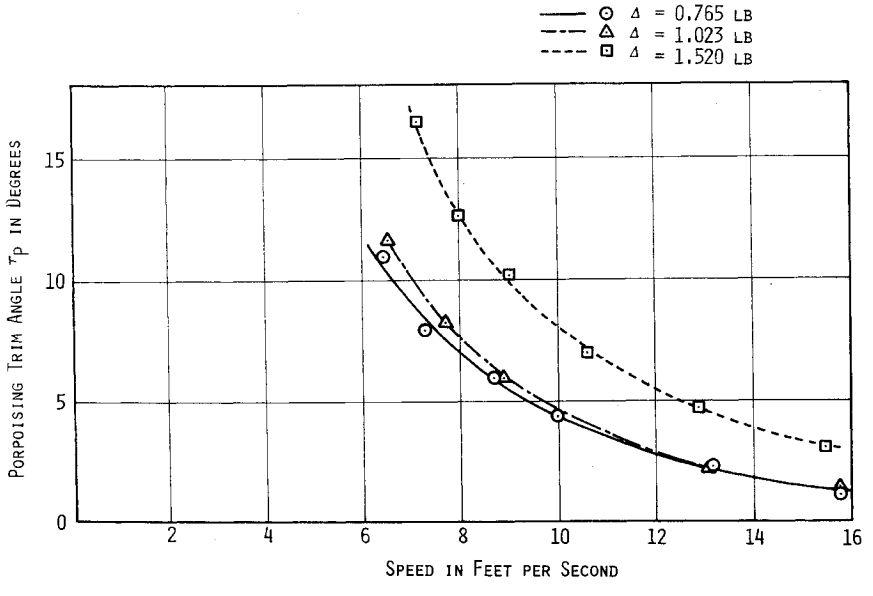

Fig. 22 Trim angle variation with speed in the Day and Haag measurements.

Conclusions

The following conclusions assume that low angle porpoising is adequately described by the heave and pitch equations and that additional degrees of freedom, as suggested by Perring and Glauert,[2] are weakly coupled.

1) Boats (or other craft equipped with a single planing surface) are not subject to porpoise instability if they a) have a high-aspect ratio wetted planing surface (better than 2 or 3); and b) have a low-pitch moment of inertia.

In such craft, the c.g. location is not important to stability. Many such craft exist; "drag boats," "flatties," and ski boats are examples which routinely obtain speeds of the order of 200 mph without porpoising. They are strictly smooth water boats, however, and cannot be operated in any kind of seaway because of intolerable pounding.

2) Boats with more slender, low-aspect ratio planing surfaces (the most widely used, because of the better seakindliness and reduced pounding in waves) will generally porpoise if the c.g. is in the vicinity of the center of pressure, denoted by $\phi = \eta$. Stability can be obtained by a) locating the c.g. near the trailing edge of the surface, or b) locating the c.g. well forward of the center of pressure, as in the analogous aerodynamic stability case.

Racing hydroplanes such as the Molanari tunnel hulls are examples of the first solution. The large up-force near the transom which is required to trim a boat with an aft c.g. is provided by a "hook" or camber near the trailing edge. Although hydrodynamically stable, this solution in-

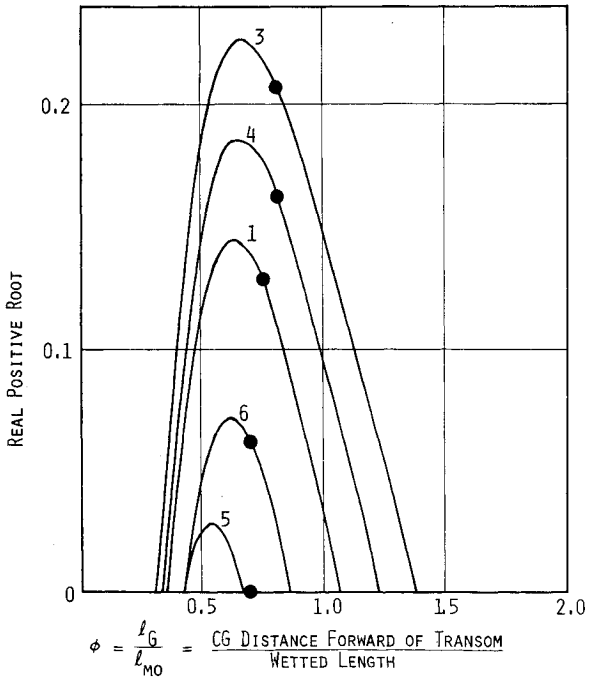

Fig. 23 Calculated damping for the Day and Haag Series 0–0.75 Tests; Runs 1–6. The Small numbers on the curves give the run number.

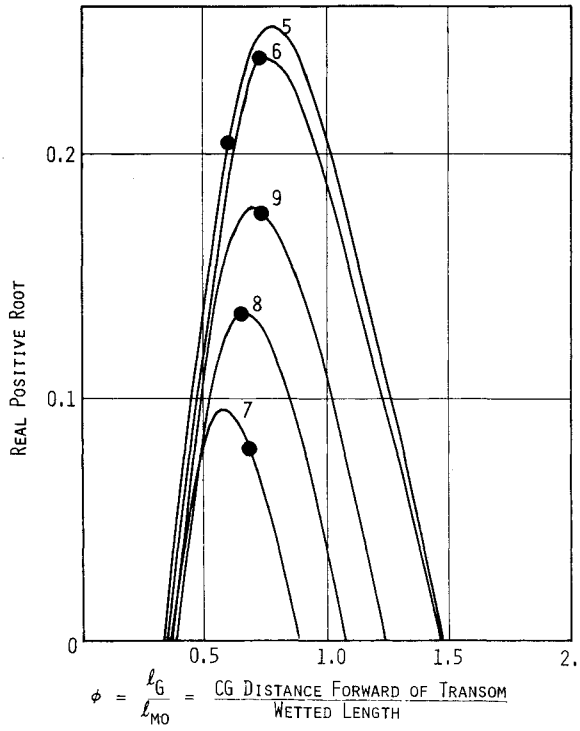

Fig. 24 Calculated damping for the Day Haag Series 0–1.0 Tests; Runs 5–9. The small numbers on the curves give the run number.

creases aerodynamic instability, because the aerodynamic center is well forward of the c.g. Also, if the forward part of the planing surface comes out of the water, the forces developed on the hook are no longer independent of the trim angle, and instability can then develop.

Stabilization by means of a forward c.g. location is employed on many boats, and is feasible because they have

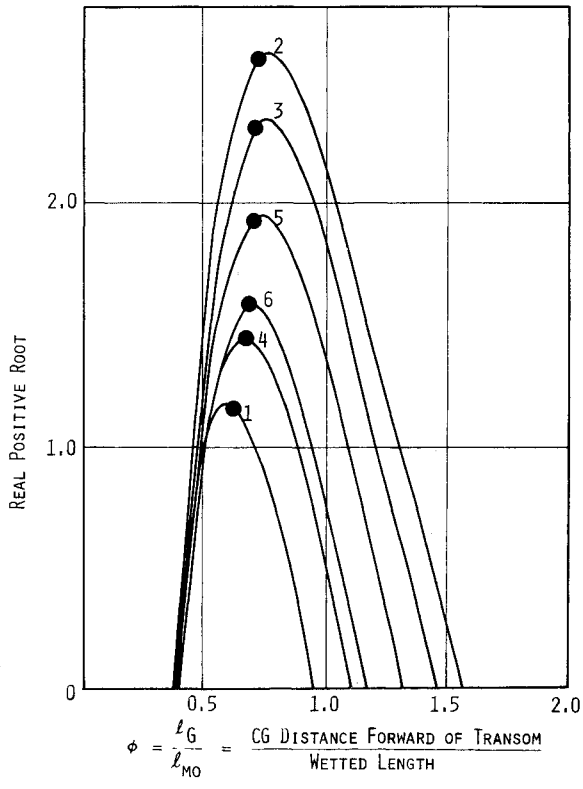

Fig. 25 Calculated damping for the Day and Haag Series 0–1.5 Tests; Runs 1–6. The small numbers on the curves give the run number.

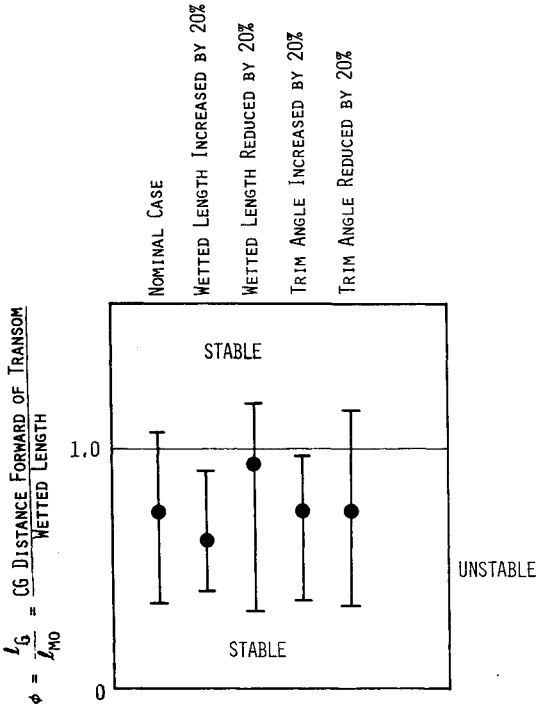

Fig. 26 The effect of measurement errors on theoretical and ±2° measured stability limits (Series 0–0.75, Run #1).

relatively high drag, so that the concomitantly large propeller thrust can provide an adequate bow-up trimming moment. Additionally, most high-speed boats of this type have outboard engines or I/O struts fitted with anti-ventilation plates, the download on which may often be a significant fraction of the boat's total displacement. The more efficient the hull, the more difficult it becomes to employ this solution.

3) One solution for an efficient high-speed boat is probably to utilize the aft c.g. zone of stabilization, and to solve the resulting aerodynamic problems separately; delta-shaped planforms and horizontal tailplanes are obvious examples of such solutions employed with seaplanes and flying boats. Both solutions have recently been employed on small boats.

4) A less obvious solution to the problem is to arrange for the boat's longitudinal radius of gyration to be very large; several times the distance (l_G) between the c.g. and the trailing edge. This then permits c.g. locations near $\phi = \eta$ to be employed so that the force penalty at the stern is small or even zero. A high speed deep-V boat planing on a small area near its transom may well be operating in this region.

5) If the geometry of a new design is at all unusual, there is no simple set of rules to avoid instability. The specific forces, moments and inertias must be calculated, and the stability evaluated as in this paper. If instability is predicted, appropriate changes in the geometry and/or moment of inertia must be made until the equations become stable.

6) Since they did not consider transient water forces in their analysis, Perring and Glauert's[2] demonstration that the horizontal degree of freedom (speed) is only weakly

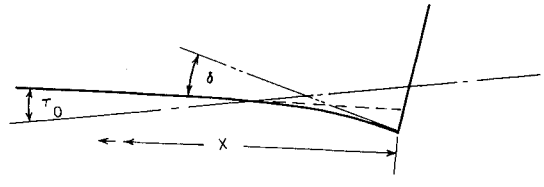

Fig. 27 Geometry of a "hooked" trailing edge.

coupled needs to be examined more closely before we can feel confident that it may be neglected in a study of porpoising instability.

7) The approach adopted in this paper can be extended to additional degrees of freedom, and to the case where the water surface is not planar; that is, to the case of motion in waves.

Appendix A

Cambered Planing Surface

Consider a slender planing surface (Fig. 27) of constant beam b. The normal forces acting upon it are given by Eqs. (27) and (29). The only term influenced by the camber is

$$\frac{dF}{dx} = m'\frac{dv}{dt} = m'u_o\frac{d\tau}{dt} = m'u_o{}^2\frac{d\tau}{dx}$$

$$\therefore \Delta F_{\text{Hook}} = m'u_o{}^2\int_{+\Delta x}^{x}\frac{d\tau}{dx}dx = m'u_o{}^2\delta = \frac{1}{8}\rho u_o{}^2\pi b^2\delta \quad \text{(A1)}$$

Comparison with the normal force equations in the main body of the paper shows that a hook of several degrees may be carrying a major portion of the boat's weight; and of course, the upload on the hook does not change with trim angle τ_o.

Equation (A1) applies to any cambered planing surface of constant width, and to "shingles" and tabs, or "boat levelers," as they are popularly known. It is of interest to note that camber generally reduces the pressure drag force on a planing surface. If the camber is obtained by a straight tab or shingle, inclined at an angle δ to the planing surface, then the (small angle) pressure drag is given by

$$D_p = \frac{1}{2}\rho u_o{}^2\pi b^2\left[C_\tau\tau_o{}^2 + \frac{\delta}{4}(\tau_o + \delta)\right] \quad \text{(A2)}$$

In contrast, if the camber is distributed continuously, as in a trailing edge "hook"

$$D_p = \frac{1}{2}\rho u_o{}^2\pi b^2\left[C_\tau\tau_o{}^2 + \frac{\delta}{4}\left(\tau_o + \frac{\delta}{2}\right)\right] \quad \text{(A3)}$$

the dynamic lift being

$$F_D = \frac{1}{2}\rho u_o{}^2\pi b^2\left[C_\tau\tau_o + \frac{\delta}{4}\right]$$

in both cases, of course.

References

[1]Savitsky, D., "Hydrodynamic Design of Planing Hulls," *Marine Technology*, Vol. 1, No. 1, Oct. 1964, pp. 71–95.

[2]Perring, W. G. A. and Glauert, H., "Stability on the Water of a Seaplane in the Planing Condition," R&M 1493, Sept 1932, Aeronautical Research Committee, Great Britain.

[3]Shuford, C. L., Jr., "A Theoretical and Experimental Study of Planing Surfaces Including Effects of Cross Section and Plan Form," Rept. 1355, 1958, NACA.

[4]Routh, E. J., *A Treatise on Dynamics of a Particle*, Dover, New York, 1898.

[5]Munk, M. M., "The Aerodynamic Forces on Airship Hulls," Rept. 184, 1924, NACA.

[6]Jones, R. T., "The Properties of Low-Aspect-Ratio Pointed Wings at Speeds Below and Above the Speed of Sound," TN 1032, 1946, NACA.

[7]Ribner, H. S., "The Stability Derivatives of Low-Aspect-Ratio Triangular Wings at Subsonic and Supersonic Speeds," TN 1423, 1947, NACA.

[8]Lamb, Sir H., *Hydrodynamics*, 6th ed., Dover, New York, 1932.

[9]Miles, J. W., "Virtual Momentum and Slender Body Theory," *Quarterly Journal of Mechanics and Applied Mathematics*, Vol. 6, No. 3, 1953.

[10]Wagner, H., "Phenomena Associated With Impacts and Sliding on Liquid Surfaces," S-302, July 1936, Aeronautical Research Committee, Great Britain.

[11]Chuang, S. L., "Slamming of Rigid Wedge-Shaped Bodies With Various Deadrise Angles," Rept. 2268, Oct. 1966, David Taylor Model Basin, Washington, D.C.

[12]Day, J. P. and Haag, R. J., "Planing Boat Porpoising," B.S. thesis, May 1952, Webb Institute of Naval Architecture, Glen Cove, N.Y.

[13]Klemin, A., Pierson, J. D., and Storer, E. M., "An Introduction to Seaplane Porpoising," *Journal of the Aeronautical Sciences*, Vol. 6, No. 8, June 1939, pp. 311–318.